Geology of western Ullsfjord, North Norway, with emphasis on the development of an inverted metamorphic gradient at the top of the Lyngen Nappe Complex

JANET COKER-DEWEY, MARK G. STELTENPOHL & ARILD ANDRESEN

Coker-Dewey, J., Steltenpohl, M. G. & Andresen, A.: Geology of western Ullsfjord, North Norway, with emphasis on the development of an inverted metamorphic gradient at the top of the Lyngen Nappe Complex. *Norsk Geologisk Tidsskrift,* Vol. 80, pp. 111–128. Oslo 2000. ISSN 0029-196X.

The Ullsfjord area of northern Troms comprises rocks from two allochthons: (1) a fragmented ophiolite complex and non-conformably overlying fossiliferous (Upper Ordovician–Lower Silurian) metasedimentary rocks (Balsfjord Group) of the Lyngen Nappe Complex and (2) exotically derived metasedimentary and meta-igneous rocks of the overlying Tromsø Nappe Complex. Tromsø Nappe Complex rocks are exposed as isolated klippen on the highest peaks in Ullsfjord. A synmetamorphic, inverted metamorphic gradient exists within the prograde assemblages of the Balsfjord Group, such that chlorite-zone assemblages occur at the base of the sequence and sillimanite-zone assemblages occur immediately beneath the thrust contact with the overlying Tromsø Nappe Complex. The entire Barrovian sequence of mineral zones, with the exception of kyanite, is present in the footwall. Complexity of rock fabrics increases sympathetically with metamorphic grade progressing structurally upwards. Simple bedding-cleavage relations at the base of the section give way upward to crenulation cleavage, transposition fabrics, schistosity and gneissosity. Relict cross-beds, graded beds and pillow basalts are stratigraphically upright. Meso- and microscopic structures record two main deformational events; D_1 resulted in prograde assemblages, and D_2 formed post-metamorphic gentle-folds. The combined structural and metamorphic data indicate thrust emplacement of a hot Tromsø Nappe Complex upon the cooler Lyngen Nappe Complex. The inverted metamorphic gradient is due to originally inverted isotherms although minor syn-emplacement reshuffling along foliation planes may have aided in the vertical stacking. An increase in shear strain approaching the nappe boundary is attributed to thermal weakening during emplacement of the Tromsø Nappe Complex. $^{40}Ar/^{39}Ar$ mineral cooling dates indicate that metamorphism and nappe emplacement occurred at ca. 432 Ma.

Janet Coker-Dewey, Mississippi State University, P.O. Box 9681, MS 39762, USA (e-mail. jdewey@cfr.mssstate.edu); Mark G. Steltenpohl, Department of Geology, 210 Petrie Hall, Auburn University, Auburn, Alabama, 36849-5305, USA; Arild Andresen, Department of Geology, University of Oslo, P.O. Box 1047, Blindern, 0316 Oslo, Norway

Introduction

The Caledonian mountain chain is a middle Paleozoic collisional orogen in which Baltic basement and its cover sediments (Lower and MiddleAllochthons) and suspect or exotic terranes comprising spreading ridges, rifted island arcs and marginal basins (Upper and Uppermost Allochthons) were thrust emplaced upon Baltica as it was partially subducted beneath Laurentia (Roberts & Gee 1985). The nappe sequence preserved in the Ullsfjord area (Figs. 1, 2), from bottom to top, includes the Nordmannvik Nappe and the Lyngen Nappe Complex of the Upper Allochthon and the Tromsø Nappe Complex of the Uppermost Allochthon (Andresen & Steltenpohl 1994). These nappes are regionally metamorphosed and show evidence of multiple deformation. The uppermost units of the Lyngen Nappe Complex, the Balsfjord Group (Bergh & Andresen 1985), locally exhibit an abrupt (<1 km), poorly understood, inverted metamorphic gradient (Fig. 3), where the highest temperatures occur immediately below the structurally overlying Tromsø Nappe Complex (Binns 1978; Humphreys 1981; Krogh et al. 1990). The inverted metamorphic gradient contains a Barrovian sequence from the chlorite-zone at lower structural levels through the sillimanite-zone at progressively higher structural levels (Humphreys 1981). The tectonically juxtaposed Tromsø Nappe Complex contains eclogites at structurally high levels, which are reported to have attained 675°C and 18 kb. pressure (Krogh et al. 1990).

The development of synmetamorphic, inverted metamorphic gradients is a topic of much discussion (Graham & England 1976; Crawford et al. 1987; Peacock 1987; Duebendorfer 1988; Hubbard 1989; Himmelberg et al. 1991; Jain & Manickavasagam 1993) and the mechanisms by which they form are not well understood. Bergh & Andresen (1985) and Krogh et al. (1990) suggest in-sequence stacking of the nappes and production of the metamorphic inversion at the top of the Balsfjord Group by downheating from the overlying Tromsø Nappe Complex. This requires two distinct metamorphic events: one producing the high P-T assemblages in the Tromsø Nappe Complex prior to its emplacement, and a second producing amphibolite-facies assemblages within the underlying Balsfjord Group contemporaneous with re-equilibration of the mineral assemblages along the contact. Alternatively, Humphreys (1981) suggests that the inverted

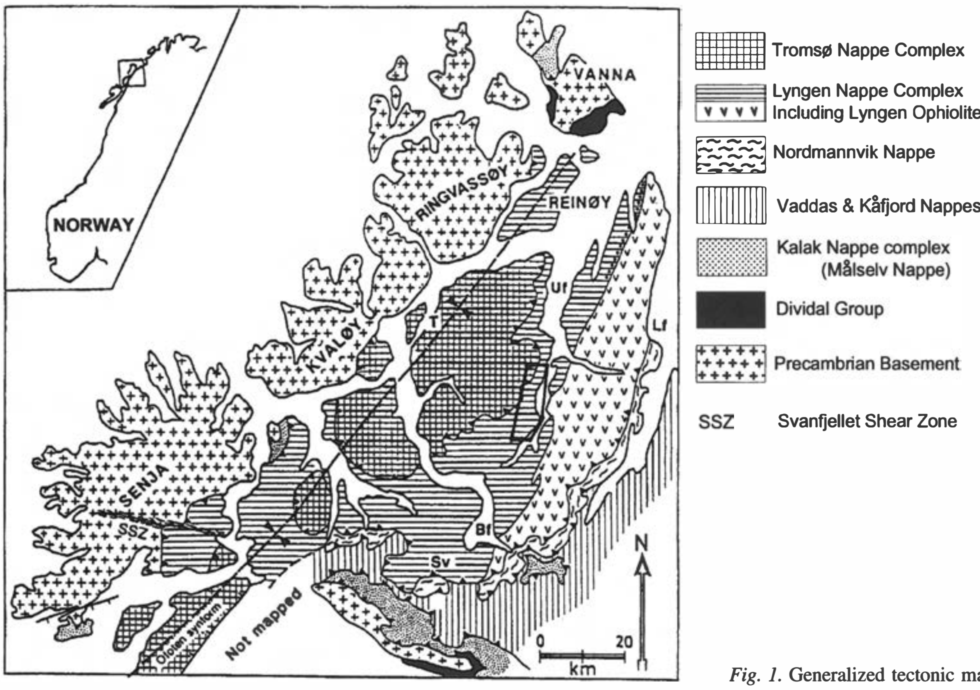

Fig. 1. Generalized tectonic map of the Troms region. From Binns (1978).

metamorphic gradient is structurally controlled by post-metamorphic thrusts within the sequence. This model requires that the metamorphic event within the Balsfjord Group occurred prior to thrusting, and may or may not be concomitant with the event that produced eclogite-facies assemblages in the overlying Tromsø Nappe Complex.

This report is the result of a detailed field investigation of 100 km^2, along the west side of Ullsfjord (Figs. 1, 2) where there is a well-exposed section through the inverted metamorphic gradient and across the boundary with the Tromsø Nappe Complex (Fig. 3). A remarkable display of fabrics and structures has developed in association with the inverted gradient. Close examination of the structures, deformational fabrics and metamorphic assemblages, coupled with $^{40}Ar/^{39}Ar$ mineral analyses on select minerals, provides constraints on the timing and development of the inverted gradient.

Large parts of the northern Caledonides are mapped only in a reconnaissance sense and information gaps have made correlation of lithologic and tectonostratigraphic units difficult in some locations. The additional information obtained from rocks in Ullsfjord permits lithologic correlation of these units with units to the west and south.

Lyngen Nappe Complex Lithologies

The Lyngen Nappe Complex contains the Lyngen Magmatic Complex (Furnes & Pedersen 1995) and unconformably overlying Balsfjord Group metasedimentary rocks (Minsaas & Sturt 1985). Balsfjord Group metasedimentary rocks include a basal conglomerate, thick (~400 m) calcite and dolomite marble sequences, mica schist, quartzite, and carbonate pebble diamictite, which are interpreted to reflect a marginal-marine shelf depositional environment (Steltenpohl et al. 1990). The Balsfjord Group provides important constraints on orogenic timing in northern Scandinavia because Late-Ordovician to Early-Silurian (Llandoverian) fossils are preserved that provide a maximum on the time of Scandian metamorphism (Bjørlykke & Olaussen 1981; Andresen & Bergh 1985; Steltenpohl et al. 1990). Some workers have reported that the Balsfjord Group contains inverted geopetal indicators in some localities (Munday 1970, 1974; Binns 1978; Binns & Matthews 1981), but others argue that there are only local areas of overturned folding and that the sequence as a whole is upright (Bjørlykke & Olaussen 1981; Andresen & Bergh 1985; Minsaas & Sturt 1985). From base to top, the Balsfjord Group in western Ullsfjord comprises graphitic phyllite interlayered with metabasalt containing some pillow structures, chloritic and graphitic phyllite and schist, interlayered with flaggy to massive quartzite, magnetite-bearing green chlorite schist, grey-and-white-banded calcite marble, massive white dolomite marble and banded metasiltstone. The metasiltstone is intruded by thin trondhjemite dikes and sills that become more common structurally upward.

Formational names were proposed by Binns & Matthews (1981) for individual Balsfjord Group units, but these have not been widely accepted by other workers (Andresen & Bergh 1985; Bergh & Andresen 1985; Andresen & Steltenpohl 1991, 1994). Informal local names are used by most authors. Because of the existing confusion in the literature with the names of formal units (Binns & Matthews 1981; Humphreys 1981; Andresen & Bergh 1985; Bergh & Andresen 1985), informal names are designated for units described herein. An attempt to associate these with more commonly used nomenclature

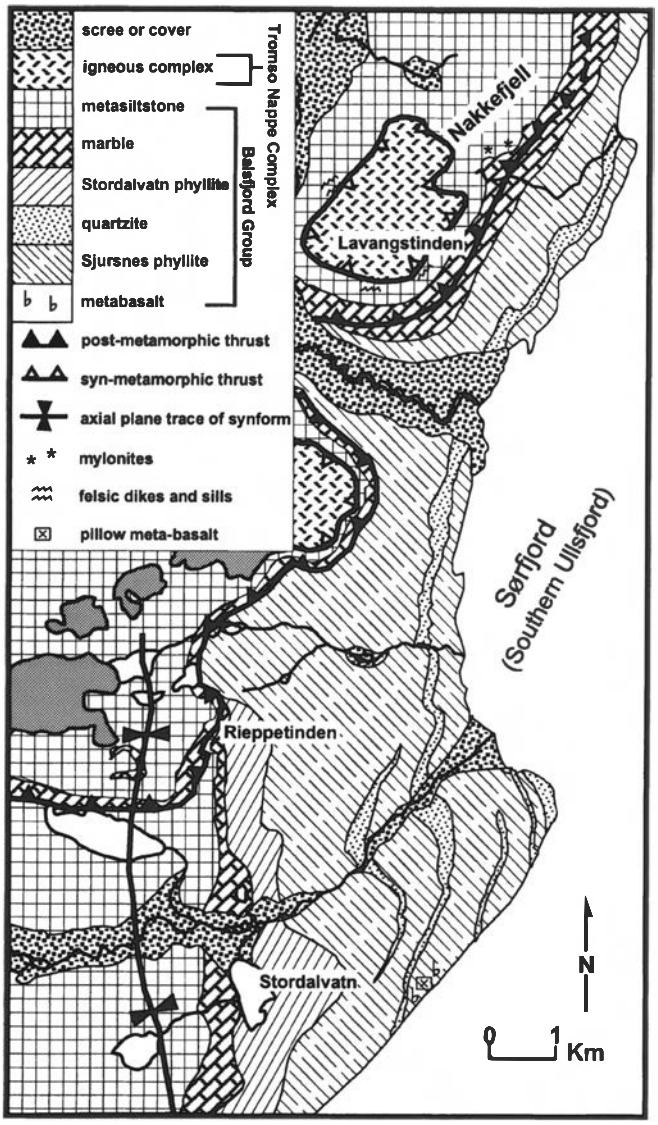

Fig. 2. Geologic map of the southern Ullsfjord (Sørfjord) area.

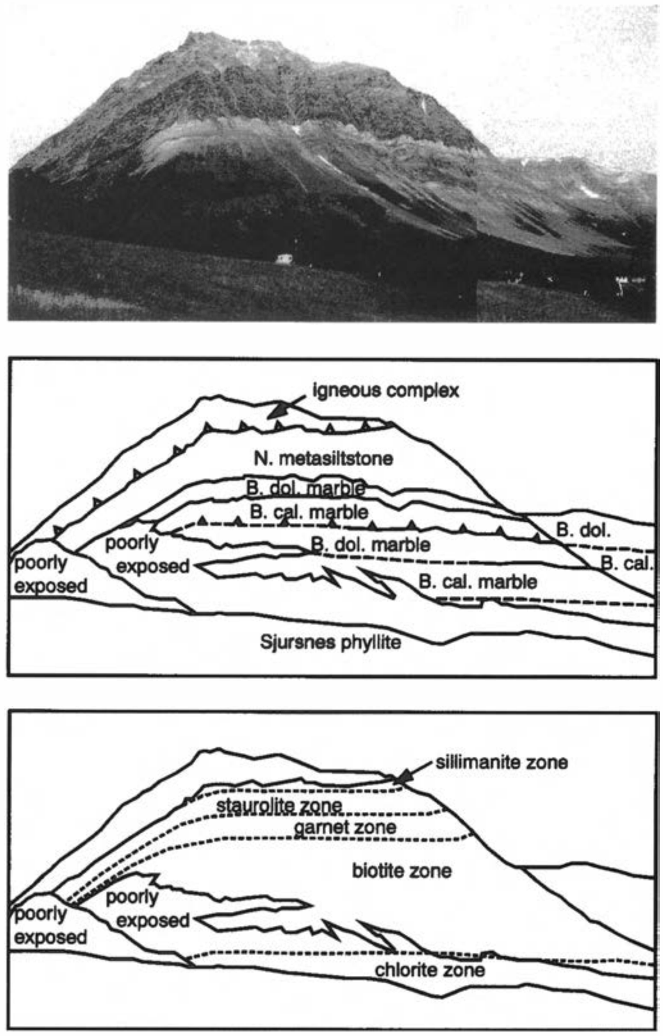

Fig. 3. View of Nakkefjell, from the shoreline facing west, illustrating structural position of lithologic units and metamorphic index minerals within the Balsfjord Group. Metamorphic zone boundaries are approximate. The photograph was taken from sea level and the mountain is 1215 m in elevation.

is made below (see section, Lithologic correlations). Lithologic descriptions will be presented in order of occurrence, from the lowest exposed units structurally upward, to the highest units. Thickness of individual units is variable owing to structural modification, and will be reported as an average. Igneous rocks are classified according to Streckeisen (1976).

Balsfjord Group metasedimentary rocks

Sjursnes phyllites. – The Sjursnes phyllites are the structurally lowest units exposed in the study area. In order of decreasing volumetric importance, this assemblage comprises a minimum of 850 m interlayered graphite and chlorite phyllite, calcite phyllite, rare thin (0.5 m thick) micaceous marble, and massive greenstone with local pillowed metabasalts and metachert. These lithologies are treated as a group because of their lithologic similarity and depositional interdigitation.

The most abundant rock near the base of the sequence is a chlorite-graphite-muscovite phyllite containing 10–40% graphite. The dominant foliation is a phyllitic cleavage which parallels compositional layering. The graphite-phyllite gradationally interdigitates with a chlorite-muscovite-calcite phyllite, which commonly has a pitted appearance in outcrop as a result of the dissolution of calcite. Locally, the calcite phyllite alternates with pale red and white bands (1–5 mm thick) of quartz and calcite marble.

Concordant, foliated greenstone lenses and layers 0.1 to 2 m thick occur throughout the Sjursnes phyllites. Principal phases are actinolite (as matrix and porphyroblasts), biotite, epidote, and plagioclase; minor consituents are quartz, chlorite, very fine-grained muscovite and opaques (including elongate white leucoxene lenses <1 mm thick). Metabasalts occur as massive, concordant, greenstone layers or lenses 0.5 to 2 m thick within the lower phyllite group at the base of the exposed section, and locally contain pillow structures, which are convex upward and tapered at the base and contain quartz-epidote filled

Fig. 4. Pillow basalt from along the shoreline at the base of the Sjursnes phyllite section. Note the convex upper margin and tapered base, indicating right way up. Light colored features are quartz-filled vesicles. Surrounding rock is interlayered chlorite phyllite, amphibolite and pale green metachert.

vesicles (Fig. 4). Primary phases include phenocrystic plagioclase (commonly altered to epidote pseudomorphs) and clinopyroxene (augite) in a fine-grained quartz-plagioclase matrix; metamorphic phases include epidote, chlorite, calcite, tremolite-actinolite, and biotite. The high graphite content of these metasediments and the occurrence of pillow basalts imply that this rock sequence was deposited in a quiet, marginal marine environment which was influenced periodically by volcanic influx. The convex-upward orientation of the pillow basalts indicates an upright stratigraphic position.

Skognesdalen quartzite. – Five quartzite units that range in thickness from <1 m to ~70 m occur within the lower phyllite group. The quartzite varies from flaggy to massive in character, with massive quartz veins up to 20 cm thick. Only one of the quartzite units appears to extend laterally throughout the entire Ullsfjord area. The upper contacts of the quartzite are gradational with the overlying phyllite, grading from flaggy quartzite interleaved with thin phyllitic bands, to quartz-rich phyllite. The unit is medium-grained, with the dominant foliation defined by fine (1 mm thick) green-grey chlorite and muscovite micaceous partings containing minor epidote, tourmaline, titanite and opaques. Pale red bands containing quartz and dolomite are 1 to 2 mm thick and graded, fining structurally upwards. Massive quartzite is bluish grey with biotite-rich micaceous partings. Crenulation fold-hinge traces are visible on some parting surfaces. Local small-scale (<0.5 cm), right-side-up cross-beds are present. A distinctive lithology at the base of the structurally highest quartzite is a black graphitic phyllite interleaved with 5-mm thick quartzite bands. The quartzite most likely represents a high-energy (shoreface?) environment, based on (1) paucity of pelitic material and (2) cross-bedding.

Stordalvatn magnetite-bearing phyllite. – Structurally above the Sjursnes phyllites is a well-foliated magnetite-bearing phyllite with quartz layers and minor, concordant, 1-m thick greenstone lenses. The unit is thickest in southeast Ullsfjord and thins toward the north; maximum calculated thickness is 100 m. The magnetite-bearing phyllite is distinctive because it contains 1–5% modal magnetite, occurring as medium- to coarse-grained (<5 mm) porphyroblasts. This unit does not appear to interdigitate with underlying units of the Sjursnes phyllite. These phyllites contain a well-developed, penetrative crenulation cleavage which has completely transposed the phyllitic cleavage as exhibited by fine micas at a high angle to the dominant foliation. A slightly more massive chlorite-muscovite phyllite containing up to 2% titanite and pyrite is associated with the magnetite-bearing phyllite, but lacks magnetite porphyroblasts. Thin (<6 cm) discontinuous layers of quartzite are common, as are vein-like quartz pods up to 20 cm thick.

Fig. 5. Top: Graded turbidites of the Nakkefjell metasiltstone. Bottom: close-up view of graded beds. Light layers contain psammitic material, whereas the dark layers contain pelitic material. Note the abrupt contact on the upper margins of pelitic layers and gradational contacts along the lower margins.

Breidvikeidet marbles. – Structurally overlying the Stordalvatn phyllite is approximately 200 m of medium-grained grey-white banded calcite marble with sparse, 1 to 50-cm thick, layers of chloritic schist and massive tremolite-actinolite-rich layers with minor intergranular quartz and tremolite. Actinolite is present in the marble, where it occurs adjacent to carbonate pelites. Pyrite and specular hematite are common; opaques are minor constituents.

Structurally above the calcite marble is approximately 150 m of relatively pure dolomite marble. The marble is fine- to medium-grained, massive, sugary textured, light grey to white in color, and usually lacks intercalated metapelites. Between the calcite and dolomite marbles is an approximately 50 m thick transitional zone in which dark grey silty marbles with micaceous partings and fine-grained grey phyllites give way to cleaner dolomite marble.

Nakkefjell metasiltstone. – Structurally, the highest metasedimentary unit of the Balsfjord Group in Ullsfjord is a distinctive ~300 m thick, sequence of banded metasiltstone and metasandstone,which is well exposed along the flanks of Nakkefjell. The Nakkefjell metasiltstone is characterized by rhythmically interbedded, relict graded beds ranging from 1 to 10 cm in thickness (Fig. 5a). The graded beds have sharp contacts at the base of psammitic layers and grade upward into fine-grained pelitic bands, indicating an upright stratigraphic orientation for this unit (Fig. 5b). These rocks are medium to coarse-grained and contain interdigitating quartz-rich muscovite-biotite schist, garnet biotite-muscovite schist, garnet gneiss and staurolite schist. At a distance, this rock is conspicuous because of its moderate brown to dark yellowish brown weathered color and the numerous felsic injections, which give the unit an appearance of being riddled with white lightning bolts (Fig. 3). Ductile deformation is indicated by isoclinal, recumbent, intrafolial similar folds, small-scale ptygmatic folds and local zones of mylonitization. Leucocratic, garnet-rich boudins are locally present. Quartz- and plagioclase-filled tension gashes are axial-planar to folds and extensional shears are locally present. Porphyroblasts of garnet and staurolite are poikiloblastic, glomeroporphyroblastic or atoll-type; sillimanite porphyroblasts are rare and occur as small cross-fractured blades within fan-shaped fibrolite. The most common mineral assemblage is garnet + muscovite + biotite + quartz ± staurolite, ± sillimanite. Minor phases may include plagioclase, hornblende, clinozoisite-epidote and chlorite. The accessory minerals titanite and ilmenite are almost ubiquitous, accounting for up to 5% of the modal mineralogy. Trace phases are apatite, allanite, and zircon.

Intrusive igneous rocks

Metagabbro. – Metagabbro crops out within the lower phyllite group as resistant, rounded knobs up to 10 m in diameter. These rocks are medium- to coarse-grained, dark green to greyish green with phenocrystic plagioclase, which is moderately saussuritized. Amphibole cleavage faces are prominent in hand sample.

Trondhjemite. – The Nakkefjell metasiltstone at the top of the Balsfjord Group contains numerous trondhjemite sills or dikes that are at a low angle to compositional layering and may either cross-cut or exhibit the regional foliation. The injections increase in abundance structurally upward and range from 10 cm to 3 m in width. The trondhjemites are medium-grained with quartz, blue plagioclase and muscovite, visible in hand sample. These rocks are inequigranular and subhedral, with graphic intergrowths of quartz and plagioclase. Plagioclase exhibits normal and oscillatory zoning, deformation twins, deformed albite twins, and ubiquitous saussuritization. Principal phases are sodic plagioclase, quartz and muscovite; minor and trace phases are chlorite, penninite, biotite, apatite, zoisite and clinozoisite.

Tromsø Nappe Complex lithologies

Tromsø Nappe Complex lithologies have been described from the type locality on Tromsø (Binns 1978; Andresen et al. 1985; Bergh & Andresen 1985; Krogh et al. 1990). Krogh et al. (1990) subdivided the Tromsø Nappe Complex into 3 main units: (1) the lower tectonic unit contains migmatized, upper-amphibolite facies, felsic gneiss, amphibolite, schist and meta-igneous rock; (2) the middle unit, the Skattøra Gneiss, comprises banded, migmatized amphibolite and amphibole gneiss cut by numerous dioritic to anorthositic dikes; and (3) the upper unit, the Tromsdalstind complex, contains schists, gneisses, marbles, and eclogites. Variably serpentinized ultramafic rocks occur locally. Field, petrological and isotopic studies of the Tromsø Nappe Complex indicate that metamorphism was multiphased (Dallmeyer & Andresen 1992). Eclogites in the upper parts have a pre- to early-Caledonian Sm-Nd mineral age (598 ± 107 Ma), whereas Silurian intrusives and mineral cooling dates throughout the nappe complex record Scandian tectonothermal activity (Krogh et al. 1990; Dallmeyer & Andresen 1992).

Binns (1978), based on a compilation of data from various workers (e.g., Padget 1955; Randall 1971; Landmark 1973; Munday 1974, and unpublished field mapping by himself, S. Bjerkenes, R. J. Humphreys, and D. W. Matthews) mapped the contact between the Lyngen and Tromsø Nappe Complexes, west of southern Ullsfjord, placing the boundary above metagabbro sheets structurally overlying the Balsfjord Group. Humphreys (1981) placed the boundary in almost the same geographic position but structurally above a 'granodiorite' within the uppermost units of the Balsfjord group. Geochemical data of Humphreys (1981) indicate variations between granitic and trondhjemitic compositions for felsic rocks above his tectonically repeated Jøvik Formation. These felsic rocks, a)

b)

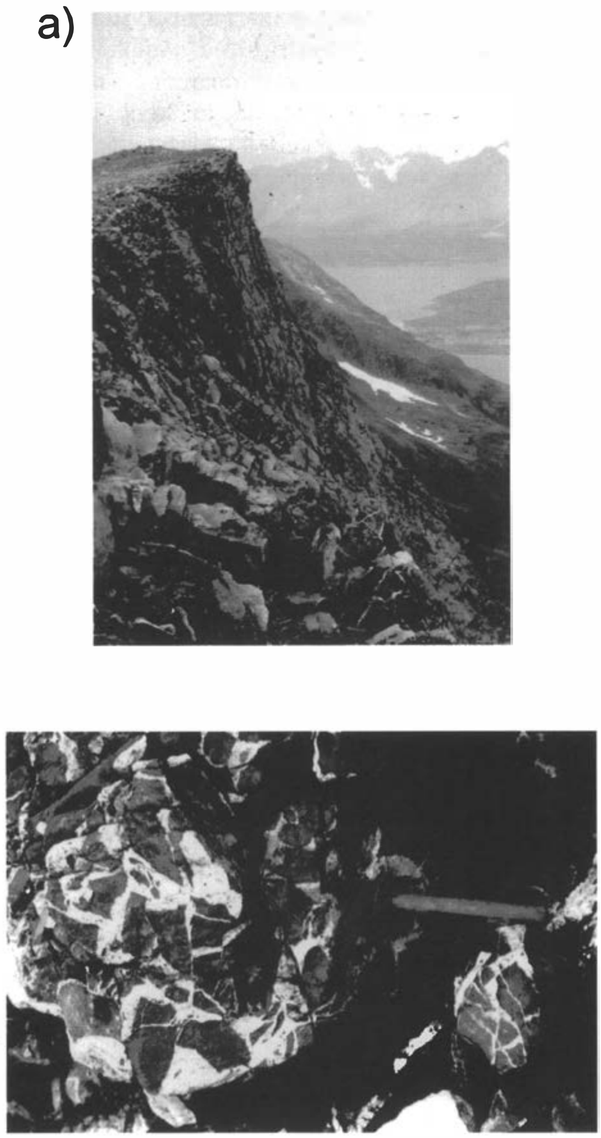

Fig. 6. Top: Igneous complex at the top of Nakkefjell. The entire cliff face (ca. 200 m relief) comprises mafic xenoliths and multiple injected felsic rock as seen in the foreground. Bottom: Close-up view of the mafic xenoliths from west Nakkefjell.

which Humphreys (1981) has grouped together as 'granodiorite and associated rocks, undifferentiated', have not been correlated with units elsewhere in Troms. Capping the highest peaks in western Ullsfjord (Figs. 3, 6), an igneous complex occurs structurally above the Balsfjord Group metasedimentary rocks and is interpreted to lie within the Tromsø Nappe Complex (see below). Zwaan et al. (1998) considered this igneous complex to be part of a separate thrust sheet, the Nakkedals Nappe, also including the Skattøra Gneiss. The contact with underlying Balsfjord Group metasedimentary rocks is fairly abrupt and, though a pronounced zone of mylonitic rock was not observed, is interpreted to be a thrust (see below). The igneous complex contains granitic gneiss, meta-pyroxenite, amphibolite, trondhjemite, and granite, which are described below in order of their relative ages of occurrence, based on cross-cutting relationships.

Granitic gneiss. – Granitic gneiss appears to be the host rock to intrusives within the igneous complex. It is pale pink to white in color, medium-grained, and locally has a well-developed banding defined by granitic domains alternating with thin muscovite and biotite partings. Locally, gneissic rocks are gradational with more massive granite bodies, implying that the gneiss locally has been mobilized; in most cases, however, granites have clearly intruded the granitic gneiss. Rare garnet + muscovite + plagioclase + quartz schists are associated with the granitic gneiss.

Meta-pyroxenite. – Plagioclase-bearing meta-pyroxenite occurs as xenoliths within the felsic rocks of the igneous complex (Fig. 6a). Texturally, the meta-pyroxenite is coarse-grained porphyritic with felsic veinlets 1 to 2 mm in width. These rocks are heterogranular with hornblende phenocrysts of up to 8 mm. Plagioclase accounts for 10–20% of the mode and is largely interstitial, although some larger relict plagioclase grains have altered to saussurite. Relict pyroxenes are rarely present as cores within larger amphibole grains and exhibit some exsolution, suggesting that the protolith may have been a gabbro-norite or a plagioclase-bearing pyroxenite. Minor phases include garnet, muscovite (after plagioclase), clinozoisite and biotite. Locally, the metapyroxenite has been sheared into amphibolite. The meta-pyroxenite and the amphibolite

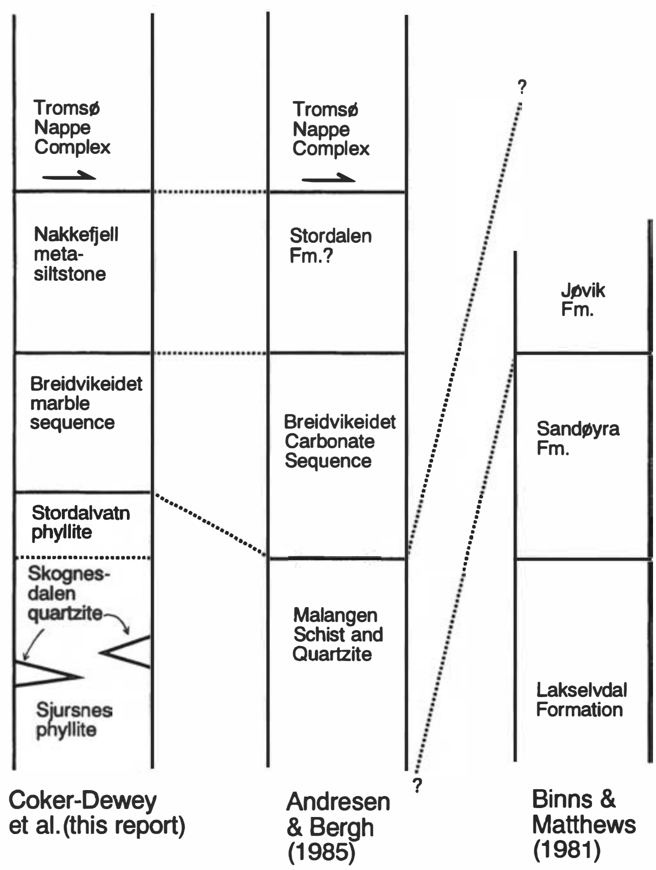

Fig. 7. Correlation between lithologic units described in this report and those described by Binns & Matthews (1981) and Andresen & Bergh (1985).

have been intruded by numerous trondhjemite injections (Fig. 6b), which have, in turn, been intruded by granitic rocks of variable composition.

Amphibolite. – Amphibolites of the igneous complex are dark green to greenish black, medium-grained, moderately well-foliated rocks with gneissic bands on the scale of <3 mm thick. They occur in outcrop as discontinuous layers <1 m thick surrounded by felsic igneous rocks. Principal phases are hornblende, garnet, plagioclase, quartz, ± biotite ± titanite. Minor phases may include zoisite, sericite and chlorite. It is possible that some of the amphibolites are sheared versions of the meta-pyroxenite.

Trondhjemite. – Trondhjemite is medium-grained and white colored with some evidence of metamorphic recrystallization. Plagioclase occurs as phenocrysts with moderately saussuritized cores. Maximum extinction angle for albite twins is 7°, indicating an oligoclase composition. Minor phases include muscovite, biotite and clinozoisite with or without interstitial microcline. Trondhjemites from the igneous complex contain potassium feldspar, whereas underlying trondhjemites in the Balsfjord Group are notably lacking in potassium feldspar. No genetic relationship between the Balsfjord Group and Tromsø Nappe Complex granitoids was established during our study, but future geochemical studies may bear this out.

Granite. – Granite is medium-to coarse-grained and pinkish grey in color. The rock is inequigranular hypidiomorphic to xenomorphic and contains myrmekitic and symplectic growths and blebby exsolution. Quartz and microcline are the dominant phases with lesser amounts of plagioclase occurring as phenocrysts with saussuritized cores. Minor phases include muscovite, biotite, garnet, epidote and clinozoisite. Strained plagioclase has deformed albite twins and microcline is commonly seen as smaller interstitial grains or in conjunction with fine-grained muscovite along plagioclase grain boundaries.

Lithologic correlations

Balsfjord Group lithologies have been described by several authors (Fig. 7) and given various names in the literature (Gustavson 1966; Binns & Matthews 1981; Bjørlykke & Olaussen 1981; Humphreys 1981; Andresen & Bergh 1985; Andresen et al. 1985; Bergh & Andresen 1985; Minsaas & Sturt 1985; Barker 1986; Steltenpohl et al. 1990; Andresen & Steltenpohl 1991, 1994). Humphreys (1981) has employed local names, after Binns (1978) and Binns & Matthews (1981), for the Ullsfjord lithologies. An attempt to develop a more consistent regional nomenclature was made by Andresen & Bergh (1985). In Fig. 7 local names used in this report are correlated to units described in Binns & Matthews (1981) and Andresen & Bergh (1985).

The lowest exposed units in Ullsfjord are the interbedded phyllites and quartzites herein called the Sjursnes phyllite and the Skognesdalen quartzite. These units are lithologically similar to the lower Jøvik Formation of Humphreys (1981). Andresen & Bergh (1985) describe an interdigitating schist and quartzite unit with minor amounts of amphibolite and garbenschiefer, which they called the Malangen schist and quartzite. Based on close lithologic similarity, it is here suggested that the Sjursnes phyllite and the Skognesdalen quartzite correspond to the Malangen schist and quartzite of Andresen & Bergh (1985). The Stordalvatn phyllite is interpreted to correspond to magnetite-bearing chlorite-carbonate schists of the Jøvik Formation (Binns & Matthews 1981; Humphreys 1981). Areal extent of the Stordalvatn phyllite appears to be limited and the unit probably does not occur in the Balsfjord area described by Andresen & Bergh (1985). The Breidvikeidet marbles of Ullsfjord are equivalent to the Breidvikeidet carbonate sequence of Andresen & Bergh (1985). Correlations with this part of the Balsfjord Group and units as far south as Ofotfjorden have been described by Steltenpohl et al. (1990) and Andresen & Steltenpohl (1991, 1994).

Correlation of the distinctive Nakkefjell metasiltstone is problematic owing to a lack of detailed descriptions of these lithologies in previous reports. Humphreys (1981) considered rocks in the equivalent position of our Nakkefjell metasilstone to be part of the Jøvik Formation, which he described as being repeated above the Sandøyra Formation by an internal thrust within the Balsfjord Group. As is clear from our descriptions above, however, lithologies of the Nakkefjell metasiltstone are distinctive and do not resemble those in any other unit in western Ullsfjord. In their study area, Andresen & Bergh (1985) describe the Stordalen Formation as a package of alternating sandstones and siltstones lying above the Breidvikeidet carbonate sequence, indicating that it is most likely equivalent to the Nakkefjell metasiltstone.

The granitic gneiss of the igneous complex of western Ullsfjord is lithologically comparable to the gneisses described from the lower parts of the Tromsø Nappe Complex (Krogh et al. 1990). Likewise, the amphibolite and cross-cutting trondhjemitic to granitic injections of the igneous complex in the highest peaks of the study area are remarkably similar to lithologies of the Skattøra Gneiss (Fig. 6). The presence of ultramafic bodies within the igneous complex is another similarity with the Tromsø Nappe Complex. The igneous complex lies in the correct tectonostratigraphic position to be correlated with the lower parts of the Tromsø Nappe Complex. Although we recognized no obvious, throughgoing zone of mylonitization associated with this tectonostratigraphic level, the boundary is abrupt and several, relatively high-temperature mylonites (crystal-plastically deformed feldspar) were observed locally in some of the granitic lithologies (see Fig. 1). Our petrography indicates only slight compositional differences between the felsic intrusives within the igneous complex and those at the top of the Balsfjord

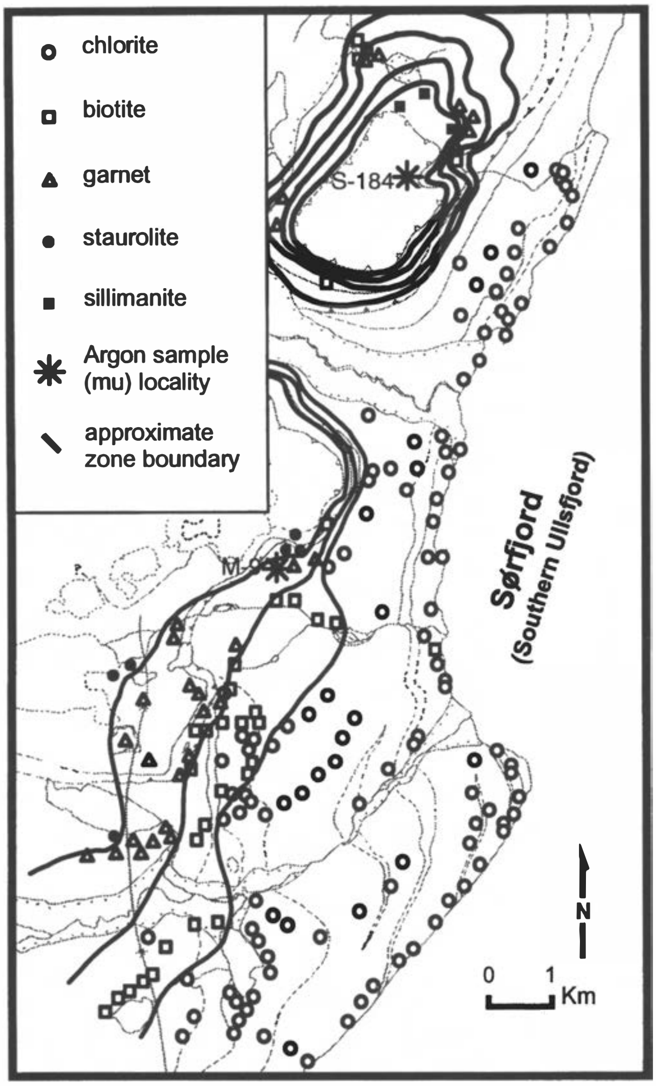

Fig. 9. Prograde index minerals observed in western Ullsfjord and their inferred zonal boundaries (see text). Greytone map is modified from Fig. 2. Sample localities for $^{40}Ar/^{39}Ar$ are also indicated.

Group. These findings, coupled with the vast differences in lithology and overall tectonometamorphic development between the Lyngen and Tromsø Nappe Complexes, lead us to favor the interpretation that the igneous complex is distinct from rocks of the Lyngen Nappe Complex and instead corresponds to parts of the lower tectonic unit and the Skattøra Gneiss of the Tromsø Nappe Complex (Figs. 2, 3).

Metamorphism and rock fabric

Eighty-nine thin sections, 60 of which came from pelitic lithologies, were analyzed petrographically in order to evaluate rock fabric and phase equilibria as they progressively change from low- to high-structural levels of the Balsfjord Group. (Because the rocks are extremely fine grained in the lower parts of the section, petrographic determination of metamorphic grade and metamorphic events at these levels is difficult.) The first metamorphic event that affected these rocks was a prograde dynamothermal one, which occurred concomitant with the first recognizable deformational event (D_1). Prograde assemblages within the Balsfjord Group record a complete, though inverted, Barrovian-type metamorphic sequence, from the chlorite zone up through the sillimanite zone, traversing structurally upward from the western Ullsfjord shoreline to the peaks lying immediately to the west (Figs. 2, 3). Retrograde metamorphism has overprinted and locally obliterated the earlier-formed prograde assemblages. Single or dual-phase multi-crystal pseudomorphs of porphyroblasts are common, particularly at the higher structural levels in the Balsfjord Group.

Balsfjord Group prograde metamorphism

Both metamorphic grade and structural complexity increase structurally upward within the Balsfjord Group and are illustratively summarized in Fig. 8. This investigated sequence has been subdivided into seven deformational/metamorphic zones containing characteristic fabrics, structures, and mineral assemblages associated with the metamorphic event. Zones A through G correspond to increasingly higher structural levels within the Balsfjord Group. The development of these zones is significant to interpreting the formation of the inverted metamorphic gradient and will be discussed further in this paper.

The distribution of prograde index minerals recognized in rocks of western Ullsfjord is presented in Fig. 9. The diagram was constructed by plotting the locations of the highest-grade index mineral observed in a given sample and contouring the data with respect to metamorphic zonations. In the diagram, lower-grade index minerals occur locally and sporadically alongside higher-grade ones within individual zones, which certainly reflects bulk compositional control. We interpret these, however, to reflect true metamorphic zonations, following the discussion (below) of observed assemblages and phase equilibria. The progression of metamorphic zones within the pelitic rocks, from chlorite zone up through sillimanite zone, occurs from the east to the west and from the base of the sequence to the top; an exception is that kyanite was not observed in this study. Right-way-up indicators such as relict cross-beds, pillow basalts (Fig. 4) and thick (several hundreds of meters), continuous sections of relict graded beds (Fig. 5) indicate that the Balsfjord Group is upright in the study area such that the structural base of the section is equivalent to the stratigraphic base of the section.

Semi-pelitic and pelitic lithologies. – Pelitic lithologies at the lowermost exposed levels of the Sjursnes phyllites commonly contain the prograde assemblage: chlorite + muscovite + quartz ± calcite ± plagioclase (albite?) ± graphite. At this structural level, the dominant foliation is the compositional layering, S_0. Incipient slaty cleavage, S_1, has developed parallel to the compositional layering and axial planar to mesoscopic folds (Fig. 8, zone A).

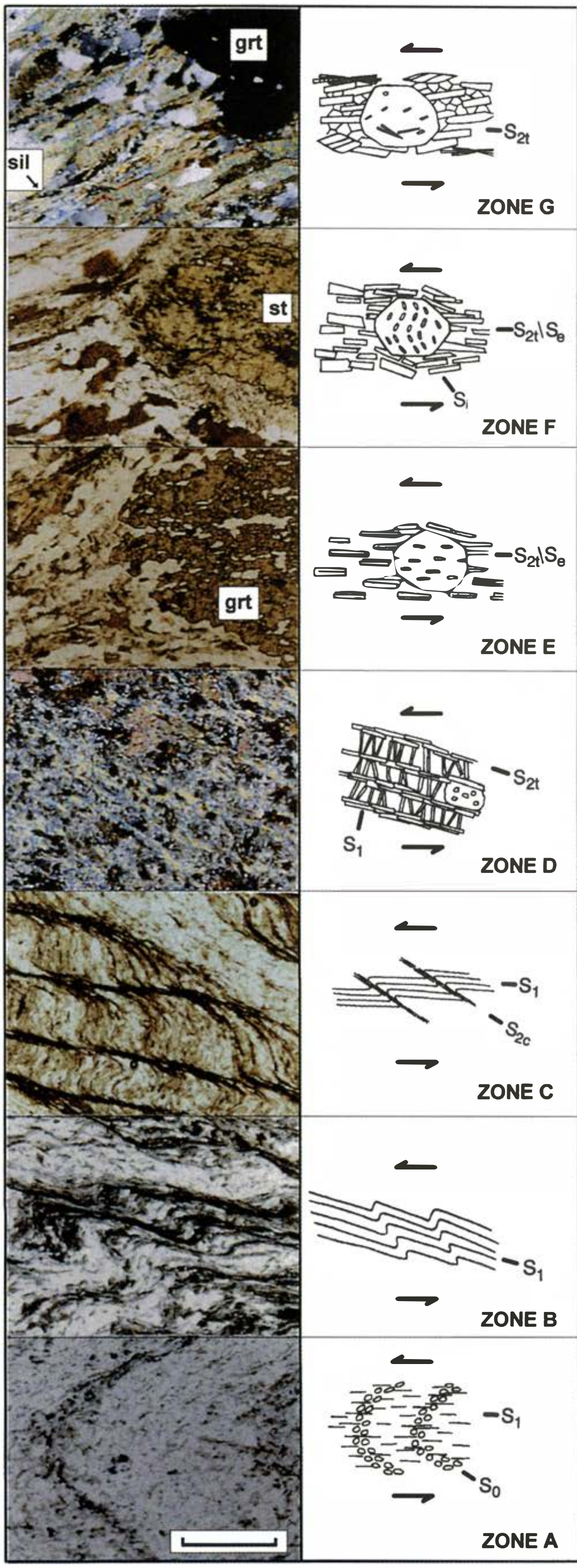

	Fabrics	Metamorphic Assemblages
ZONE G	schistosity / gneissic banding sillimanite needles garnet porphyroblasts granular texture	Sil + Grt + Ms + Bt + Pl + Qtz Grt + Ms + Bt + Pl + Qtz
ZONE F	schistosity garnet & staurolite porphyroblasts Si inclined to Se	St + Grt + Ms + Bt + Qtz + Plag Grt + Bt + Ms + Pl + Qtz
ZONE E	phyllitic cleavage schistosity garnet porphyroblasts Si parallel to Se	Grt + Bt + Ms + Pl + Qtz Grt + Bt + Ms + Zo + Qtz Grt + Bt + Ms + Qtz
ZONE D	transposition phyllitic cleavage schistosity biotite porphyroblasts	Bt + Ms + Pl + Ep + Qtz Act + Bt + Ms + Czo + Qtz Chl + Ms + Czo + Qtz Chl + Ms + Ab + Qtz + opaques
ZONE C	spaced crenulation cleavage phyllitic cleavage	Chl + Ms + Cal + Qtz + opaques Chl + Ms + Qtz + opaques
ZONE B	crenulation phyllitic cleavage	Chl + Cld + Ms + Qtz + graphite Cld + Ms + Cal + Qtz + graphite Chl + Ms + Qtz + graphite
ZONE A	slaty cleavage phyllitic cleavage	Chl + Ms + Cal + Qtz + Ab Chl + Ms + Qtz + graphite

Fig. 8. Deformational fabrics and metamorphic mineral assemblages of the prograde metamorphic event. Schematic drawings illustrate the progression moving structurally upward. Scale bar = 0.5 mm. See text for further explanation.

At structurally higher levels, the phyllites become crenulated and develop an incipient, spaced crenulation cleavage which is oblique to the compositional layering (Fig. 8, zones B, C). The dominant metamorphic assemblage is chlorite + muscovite + quartz ± chloritoid ± calcite ± plagioclase (albite?) ± graphite. This assemblage is indicative of the chlorite-zone. The presence of chloritoid is due to bulk chemistry, reflecting a high Fe/Mg ratio. A possible chloritoid-producing reaction in these rocks is Fe-Chl + Prl = Fe-Cld + Qtz + H_2O (Spear 1993)

The incipient crenulation cleavage becomes a well-developed spaced crenulation cleavage, S_{2c}, at higher structural levels (Fig. 8, zone C). The dominant mineral assemblage at this level is chlorite + muscovite + quartz ± calcite + opaques.

Toward higher structural levels, the spaced cleavage becomes a transposition foliation, S_{2t}, in which microlithons preserve only relicts of the original fabric. Grain size of the micas increases, and biotite porphyroblasts first appear (Fig. 8, zone D). The dominant metamorphic mineral assemblage is biotite + muscovite ± chlorite + plagioclase + quartz + opaques. The mineral assemblage associated with carbonate-rich pelites is biotite ± muscovite ± clinozoisite ± actinolite + quartz. Biotite porphyroblasts contain coronal quartz symplectite textures indicating solid-state exsolution. A possible reaction for the production of biotite is: Chl + Kfs = Mu + Bt + Qtz + H_2O (Spear 1993).

At higher structural levels, the transposed S_1 fabric has been rotated into the plane of the S_{2t} fabric, which at this level is a moderately well-developed schistosity (Fig. 8, zone E). Garnet first appears at this structural level. S_{2t} is preserved in garnet porphyroblasts that have an internal schistosity parallel to the external schistosity (Fig. 8, zone E). Some remnants of the transposed S_1 phyllitic cleavage are visible in the domains between S_{2t} foliation traces. A significant increase in grain size is apparent both in the porphyroblasts and in the matrix phases. The dominant mineral assemblage at this structural level is garnet + biotite + muscovite + quartz ± plagioclase ± zoisite ± clinozoisite.

At the first appearance of staurolite, which occurs at a still higher structural level, the rock fabric begins to take on the appearance of a true schistosity (Fig. 8, zone F). The fabric is coarse grained with euhedral biotite, garnet and staurolite porphyroblasts. Quartz subgrains and new grains become prominent, as do quartz-quartz triple-point junctions. Little of the pre-existing transposed S_1 foliation is recognizable, except where it occurs as an internal schistosity (S_i) in porphyroblasts. In Fig. 8, zone F, the staurolite porphyroblast contains an internal fabric, appearing as opaque inclusions, which is at an angle to the metamorphic schistosity (S_{2t}) of the matrix surrounding the porphyroblast.

The most common equilibrium assemblages at this structural level are (1) staurolite + garnet + muscovite + biotite + quartz, (2) garnet + muscovite + biotite + plagioclase + quartz and (3) garnet + biotite + staurolite + clinozoisite + quartz. These assemblages indicate the achievement of staurolite-zone conditions. Because staurolite is not found in the same lithology in which chloritoid occurs and chloritoid is only a minor phase, it is unlikely that staurolite production occurred as a result of chloritoid consumption. A likely staurolite-producing reaction for these rocks is therefore Chl + Ms = St + Bt + Quartz + H_2O.

Another important reaction, one that marks the first appearance of the paragenesis staurolite + biotite in low-Al pelites, is: Grt + Chl = St + Bt + H_2O (Spear 1993).

At the structurally highest level, immediately beneath the thrust at the base of the igneous complex, sillimanite appears as growths around the margins of garnet porphyroblasts (Fig. 8, zone G). The predominant rock fabric at this level is a schistosity, but locally, differentiation is advanced and a gneissosity has formed. Pre-existing foliations are no longer discernable at this level except as S_i fabrics within porphyroblasts. Common pelitic assemblages at this structural level are (1) sillimanite + garnet + muscovite + biotite + plagioclase + quartz, and (2) garnet + muscovite + biotite + plagioclase + quartz. Hoschek (1969) has suggested that staurolite breaks down according to the reaction St + Ms + Qtz = Al_2SiO_5 + Bt + H_2O and occurs within a range of 2–5.5 Kb H_2O pressure and 575–675°C, depending on the magnesium content of staurolite. The terminal stability reaction for staurolite in the KFMASH system St = Grt + Bt + Sil + H_2O may be responsible for staurolite breakdown as sillimanite is produced (Spear 1993).

Non-pelitic lithologies. – The overall trend of increasing metamorphic grade with higher structural level is also observed in higher variance assemblages of metamorphosed mafic and calcareous rocks. Mafic rocks of the Sjursnes phyllites at the base of the section are either greenstones or chlorite phyllites containing the assemblage chlorite + muscovite + quartz + actinolite + epidote + magnetite, indicating greenschist-facies conditions. At higher structural levels (that is above the Breidvikeidet marble), the rocks become amphibolites and gneisses. The mineral assemblage at the highest structural levels within the igneous complex is hornblende + quartz ± garnet ± plagioclase ± biotite, indicating amphibolite-facies conditions.

Siliceous marbles of the Sjursnes phyllite at mid-structural levels are predominantly calcite or dolomite marbles containing tremolitic amphiboles, most likely produced by the general reaction: Dol + Qtz = Tr + Cal.

Temperatures for this reaction range from 500 to 600 °C for 5 kbar and $X_{CO_2} \sim 0.12$ to 0.9 (Spear 1993).

Immediately beneath the igneous complex, at the highest structural levels within the Balsfjord Group, marbles contain diopside porphyroblasts. A possible diopside producing reaction is:

$$Tr + Cal = Di + Dol + CO_2 + H_2O.$$

The temperature for this reaction is ~660°C at 5 kbar and Xco_2 ~0.5 (Spear 1993), which is in agreement with the sillimanite zone assemblages of pelites within the Nakkefjell metasiltstone.

The Sjursnes phyllite, the Stordalvatn magnetite-bearing phyllite and the Nakkefjell metasiltstone are relatively titanium-rich rocks. At lower and middle structural levels, phyllites contain the phases ilmenite, leucoxene and titanite. Within the sillimanite zone, the dominant titanium-bearing phase is rutile, which occurs as needles in biotite, hornblende and almandine, suggesting high P-T conditions (Deer et al. 1991). These relationships also indicate increasing metamorphic grade with higher structural levels.

Syn-kinematic trondhjemite injections that are absent below the Nakkefjell metasiltstone, but increase in abundance structurally upward within it, may have formed as a result of partial melting of this unit. If these injections are *in situ* partial melts, temperatures may have exceeded about 650°C at pressures of up to 6–7 kbar, considering that sillimanite is the stable Al_2SiO_5 phase in the metasiltstone (Spear 1993). Although these relations would be consistent with upward increasing metamorphic conditions, we did not observe migmatites or any other evidence for partial melting in the metasiltstone. Future petrologic studies of these injections, and the rocks from the local areas where the granitic gneiss within the overlying igneous complex has been mobilized, are planned in order to explore the significance of these relations for the development of the inverted metamorphic gradient.

Balsfjord Group retrograde metamorphism

Retrogression is indicated by the partial or complete replacement of porphyroblasts by phases of lower metamorphic grade. Generally, there is no fabric associated with the retrogression. Rarely, a fine-grained axial-planar fabric has developed in conjunction with the retrograde assemblage chlorite + epidote + quartz. Although retrogression is pervasive on a mesoscopic scale, the degree of retrogression is variable in terms of both areal extent and structural level. In garnet-staurolite 2-mica schist from upper structural levels of the Balsfjord Group, garnet porphyroblasts are replaced by chlorite along fractures and biotite has been completely replaced by chlorite *in situ* as pertains to the fabric. Multi-crystal sericite pseudomorphs after staurolite are ubiquitous and in most samples no relict staurolite is preserved (Fig. 8, zone F). Humphreys (1981) called these pseudomorphs 'shimmer aggregate'. Garnet retrogression is extremely variable from pristine-unaltered to near complete pseudomorphism by chlorite. Chlorite intergrowths in biotite porphyroblasts are also common.

Tromsø Nappe Complex metamorphism

Metamorphism in rocks of the Tromsø Nappe Complex exposed in the study area achieved amphibolite-facies conditions. The paucity of pelitic rocks and the limited bulk compositions of the granitic gneisses and metaplutonic rocks, however, make it difficult for us to constrain the conditions of the metamorphic peak more tightly. Rare schists contain garnet + muscovite + plagioclase + quartz, and granitic gneisses and granite contain plagioclase + K-feldspar + biotite + muscovite ± garnet, which exist over a broad range of conditions and thus are not diagnostic of metamorphic grade. Amphibolites contain the assemblage hornblende + garnet + plagioclase + quartz + titanite ± biotite, which is characteristic of the amphibolite facies (Carmichael 1978; Spear 1993). The lack of metamorphic pyroxene in the granitic gneisses and garnet amphibolites indicates that metamorphic conditions achieved in these rocks were considerably lower than the granulite- and eclogite-facies conditions reported in rocks from the higher parts of the Tromsø Nappe Complex exposed in the Tromsø area (Krogh et al. 1990). We note, however, that our observations on the rocks of the igneous complex are limited and that our samples reflect conditions from only the most basal levels of the Tromsø Nappe Complex directly adjacent to the thrust boundary with the Balsfjord Group.

Mesoscopic structure

On the basis of measured structural and fabric elements and petrography, two phases of deformation, herein referred to as D_1 and D_2, are recognized in the Lyngen Nappe Complex of the study area. The fabrics and metamorphic assemblages are considered progressive features that vary with structural level. The first deformational event, D_1, was synchronous with prograde metamorphism and produced an S_1 regional phyllitic cleavage, an S_{2c} spaced crenulation cleavage and an S_{2t} transposition foliation at successively higher levels within the section. Mesoscopic folds deform these foliations but are considered to have formed at late stages during the progressive D_1 event. Mesoscopic structures vary with tectonostratigraphic level and will be described in order of their occurrence from the base to the top of the section. F_1 folds that deform S_1 but still belong to the D_1 phase of deformation are referred to as post-S_1 folds.

At the base of the Balsfjord Group section studied, S_1 slaty cleavage occurs axial-planar to folds of compositional layering, S_0 (Fig. 10a). S_1 dips mainly to the west–northwest at about 30° and is weakly folded about axes plunging gently to the north–northwest (Fig. 11a, b). Progressing upward, the slaty cleavage develops into a phyllitic cleavage (S_1) generally parallel to the compositional layering (S_0) (Fig. 8b). A locally penetrative crenulation cleavage (S_{2c}) overprints S_1 at low- to mid-structural levels within the Balsfjord Group (Fig. 10b). Post-S_1-fold-hinges define weak point-maxima and a partial girdle, whose pole generally corresponds to the S_0/S_1 point-maximum (Fig. 11b). In the field, post-S_1-folds are mainly crenulation folds, open- to closed-similar folds and north–south trending, east-vergent sheath folds inter-

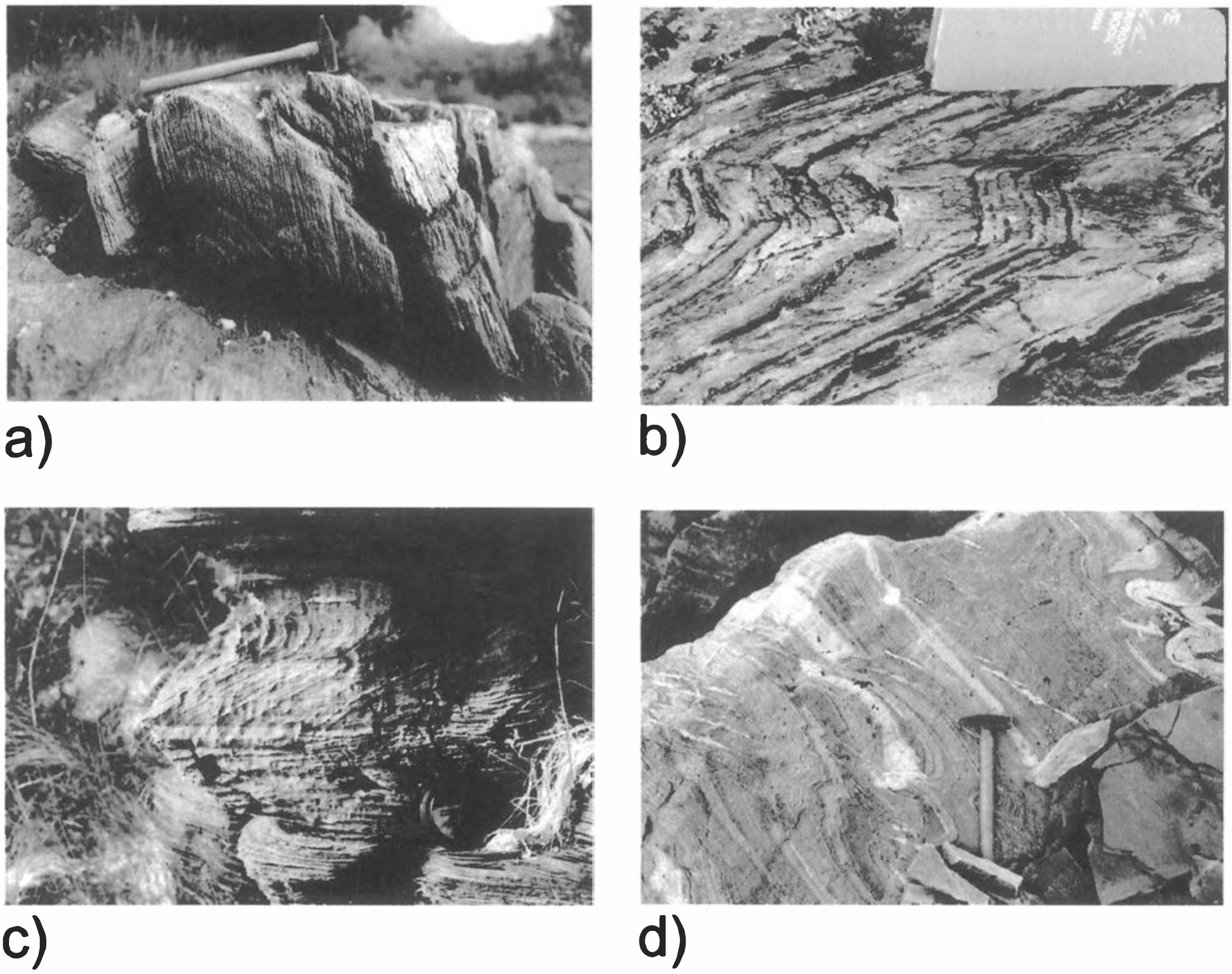

Fig. 10. Structural relationships of mesoscopic folds from the base of the Balsfjord Group section to progressively higher levels. a. Bedding (S_0) with axial-planar cleavage from along the shoreline. b. Axial-planar crenulation cleavage (S_{2c}), located structurally above photo (a). c. Incipient transposition foliation (S_{2t}) directly beneath the Breidvikeidet Marble and structurally above (a) & (b). d. Folded, crenulated and ductilely deformed Nakkefjell metasiltstone.

preted to have formed during eastward emplacement of the Tromsø Nappe Complex. Post-S_1 fold-hinge surfaces define a weak partial girdle that roughly parallels a partial girdle of S_0 and S_1 foliations (Fig. 11c).

S_{2c} is oriented at various angles to S_1, depending on the tightness of the crenulations (Fig. 11d). This resulted in the spread of S_{2c} crenulation cleavage measurements that have only a weak point-maximum, plunging shallowly toward the west (Fig. 11d). At higher structural levels S_{2c} becomes a transposition foliation (Fig. 10c) and, where intensely developed, is rotated back into the plane of S_1, defining a point-maximum corresponding to the point-maximum defined by S_0 and S_1 (Fig. 11a). Intersection lineations between S_1 and S_{2c}, and S_1 and S_{2t} define a shallow, N–S trending point-maximum (Fig. 11e). At the highest structural levels, flow folds (Fig. 10d), boudins and ductile shear zones have a distinct plastic character, consistent with deformation under increasingly higher grades of metamorphism.

The second deformation event, D_2, post-dated the peak, prograde metamorphism as indicated by a gentle warping of D_1 fabrics and structures. S_0/S_1 poles define a full girdle, which is folded about a shallow, north-plunging axis (Fig. 11a). This axis corresponds to a late, open macroscopic synform located at the southern end of the field area (Figs. 2, 11a). A second partial girdle indicates folding about a north–northwest plunging axis. F_2 folds deform earlier-formed fold-hinge surfaces about the same shallow north-plunging axis (Fig. 11c), indicating that these are the latest-formed folds. S_{2t} transposition has a similarly oriented girdle (cf., Figs. 11e, f), indicating formation prior to D_2 folding.

Geochronology

The main phase of the Caledonian deformation in Scandinavia, the Scandian phase (Gee 1975), took place at around 450–400 Ma. Previously reported isotopic age determinations in Troms support the interpretation that the Scandian was predominant. Dallmeyer & Andresen (1992) reported $^{40}Ar/^{39}Ar$ hornblende and muscovite cooling ages

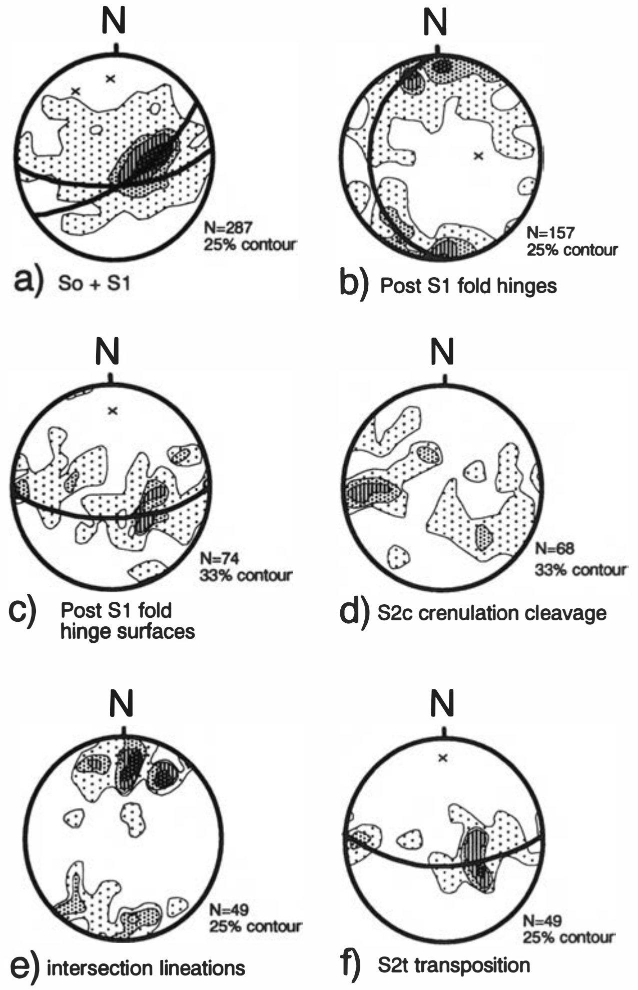

Fig. 11. Contoured equal area, lower hemisphere projections from the Ullsfjord area. All planar fabrics are plotted as poles to planes.

of 427–417 Ma for Lyngen Nappe Complex lithologies, and 481–432 Ma for Tromsø Nappe Complex lithologies which were interpreted to reflect Scandian and pre-Scandian tectonism, respectively. Krogh et al. (1990) reported a 433 ± 11 Ma Rb-Sr whole-rock isochron from a gneiss within the upper part of the Tromsø Nappe Complex. Conventional K-Ar dating of amphiboles from retrograded eclogites of the upper Tromsø Nappe Complex, and phenocrysts from an oligoclasite dike and porphyroblasts in the Skattøra gneiss of the lower Tromsø Nappe Complex have been dated at 437 ± 16, 448 ± 20 and 436 ± 20 Ma, respectively (Krogh et al. 1990).

One $^{40}Ar/^{39}Ar$ incremental-release age spectrum on metamorphic hornblende and two on muscovite were generated in an attempt to characterize the timing of metamorphism of rocks in the study area (Fig. 12). The isotopic analyses were performed using M. Kunk's laboratory, U.S.G.S., Reston, Virginia. Raw data for the analyses and a discussion of the analytical techniques and argon closure temperature estimates used for hornblende and muscovite (~500 and 375 °C, respectively) are presented the the Appendix.

Sample S-184 is a hornblende from an amphibolite within the igneous complex at the base of the Tromsø Nappe Complex. Owing to the very small amount of hornblende concentrated from this sample, 100% of ^{39}Ar gas was released in only two steps, defining a discordant spectrum with a minimum age increment of 450 Ma. Amphiboles from the north Norwegian Caledonides commonly contain excess nonradiogenic ^{39}Ar (Hodges 1985; Tilke 1986; Dallmeyer 1988; Coker et al. 1992, 1995; Coker 1993), which normally degasses at low temperature increments. Because sample S-184 degassed over such a narrow temperature range, the possible effects of extraneous argon cannot be determined, thus the 450 Ma increment is only loosely interpreted as a maximum cooling age.

Muscovite S-184, from the igneous complex granite, displays a concordant plateau and correlation age of 441 ± 2 Ma. Muscovite M-9, from a garnet-muscovite-biotite schist within the Nakkefjell metasiltstone, has a plateau age of 432 ± 2 Ma; the large uncertainty in release step five was due to an electronic problem during the 1150°C increment. This sample was collected from first idioblastic separable muscovites which occurred structurally beneath the first appearance of staurolite (Fig. 9). Sutter et al. (1985) argued that $^{40}Ar/^{39}Ar$ dates on hornblende from staurolite zone rocks approximate the time of the peak of metamorphism because they crystallized near their temperature of closure. Using similar reasoning, the date on muscovite sample M-9, which crystallized at temperatures lower than those of the overlying staurolite zone rocks, may not grossly underestimate the time of metamorphism of the Balsfjord Group.

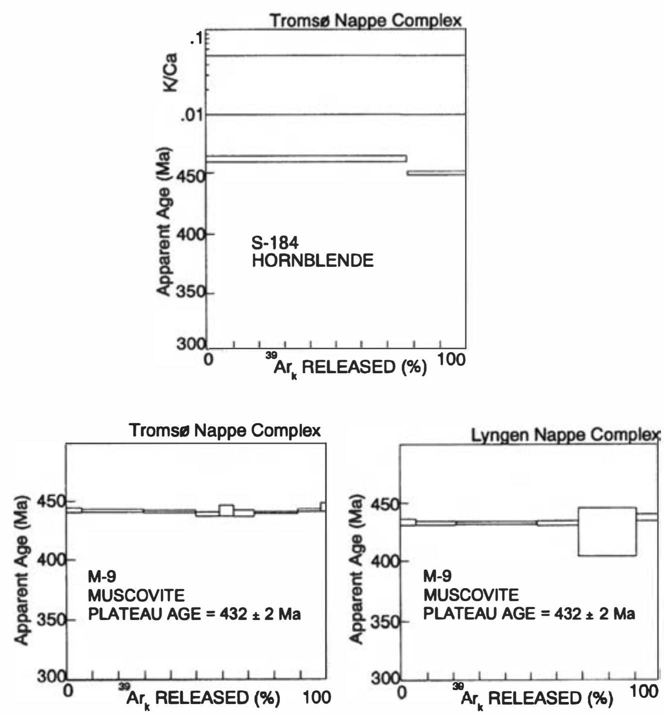

Fig. 12. Hornblende and muscovite age spectra from Ullsfjord. See Fig. 9 for sample locations. See text.

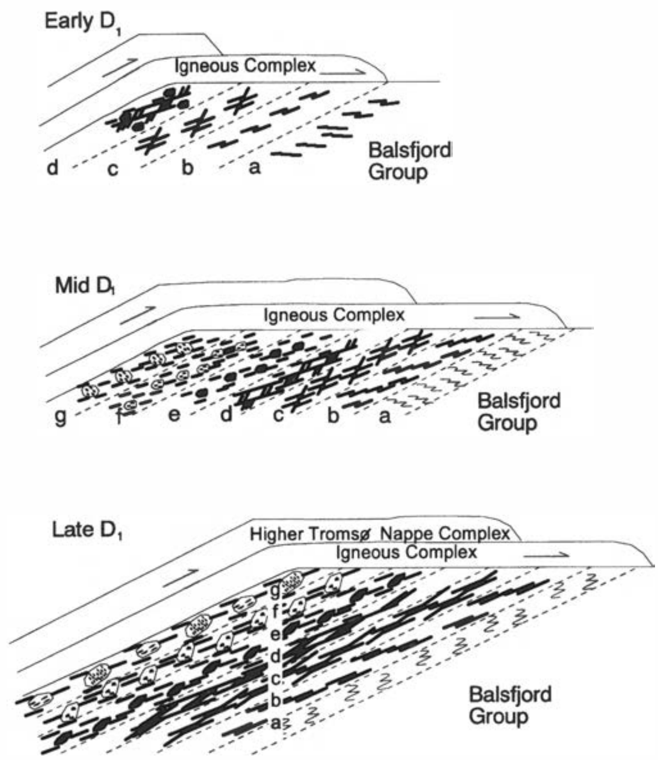

Fig. 13. Tectonic model for the development of the Lyngen Nappe Complex inverted metamorphic gradient. Lateral and vertical distances are schematic and not to scale. Zones correspond to those illustrated in Fig. 7 and described in the text. Right simple shear has been applied to the lower diagram to illustrate how fabrics might be displaced along foliation planes.

This date is consistent with the Early Silurian fossils from the Balsfjord Group (Bjørlykke & Olaussen 1981) which constrain a maximum age for metamorphism, and a 432 ± 7 Ma Rb-Sr isochron date on syntectonic metagranites that intruded the same Balsfjord Group levels on neighboring Reinøy (Lindstrøm & Andresen 1995; Fig. 1).

In summary, the $^{40}Ar/^{39}Ar$ incremental release age for hornblende in the Ullsfjord area is suspect owing to the possibility of excess argon. Muscovite plateau ages of 432 ± 2 and 441 ± 2 Ma from the Lyngen and Tromsø Nappe Complexes, respectively, are consistent with ages reported by Dallmeyer & Andresen (1992) and Krogh et al. (1990). Cooling through muscovite closure temperature in rocks of the igneous complex at the base of the Tromsø Nappe Complex is here interpreted to have occurred as a result of uplift and unroofing prior to 441 Ma. The 432 Ma age of M-9 may approximate the time of peak metamorphism in Balsfjord Group rocks of the study area.

Discussion

Our field and petrographic observations from western Ullsfjord clearly indicate that post-metamorphic folding and faulting are too weak to have played any major role in the formation of this inverted metamorphic gradient. The most commonly invoked mechanisms for the development of synmetamorphic, inverted metamorphic gradients are: (1) downheating from the emplacement of a hot upper plate (Wagner & Srogi 1987; Duebendorfer 1988; Hubbard 1989); (2) emplacement of hot magmatic bodies and subsequent contact metamorphism of the rocks below the intrusion (Hubbard & Harrison 1989; Himmelberg et al. 1991); and (3) inversion of isotherms within a subduction zone (Peacock 1987, 1988; Peacock & Norris 1989). England & Molnar (1993) and Ruppel & Hodges (1994) discuss how dissipative shear heating along thrust faults may contribute to the formation of synmetamorphic, inverted metamorphic gradients. The inverted metamorphic gradient below the Lyngen–Tromsø thrust in Ullsfjord is compressed into a <1 km zone and clearly resulted from prograde dynamothermal metamorphism, precluding post-emplacement heat-transfer as a sole mechanism. The unconformity separating the Lyngen Magmatic Complex from the Balsfjord Group, indicates that ophiolite obduction occurred prior to deposition of the Balsfjord Group (Coker et al. 1992, 1995; Andresen & Steltenpohl 1994). The presence of this unconformity, coupled with the absence of high-pressure metamorphic assemblages, appears to preclude a subduction mechanism.

Two models have been suggested for the development of the inverted metamorphic gradient in the Balsfjord Group. Humphreys (1981) suggested structural control by post-metamorphic folding and tectonic sliding whereby nappes from deep-crustal levels were brought up and emplaced upon nappes derived at shallow-crustal levels along an in-sequence imbricate thrust zone. This model requires considerable translation of individual thrust domains in order to telescope the observed metamorphic zones and does not appear to be warranted by the geologic relations. Right-way-up indicators within the Balsfjord Group in western Ullsfjord indicate that the stratigraphic sequence is not overturned, in contrast to reports by Humphreys (1981). Some local repetition is evident in a tectonic slide within the Breidvikeidet Marble but discrete retrograde mylonite zones necessitated by the imbricate thrust model were not recognized in the study area.

Krogh et al. (1990), on the other hand, suggested stacking of the nappes from top downward (in sequence), such that still hot nappes were emplaced upon the cooler ones, and downward heat transfer produced the inverted metamorphic gradient. Some workers argue that downheating alone is insufficient to produce the temperatures necessary for kyanite- and sillimanite-grade assemblages (Graham & England 1976; Wagner & Srogi 1987; Duebendorfer 1988; Hubbard 1989; England & Molnar 1993). Additional heat may have been provided during nappe emplacement by synkinematic trondhjemite injections that increase in abundance structurally upward within the Nakkefjell metasiltstone. Unfortunately, the origin of these trondhjemite injections remains to be explored. Metamorphic assemblages and fabrics in the Balsfjord Group at Ullsfjord clearly demonstrate, however, prograde dynamothermal metamorphism and therefore a simple downheating model is insufficient to explain the inversion.

It is more likely that a combination of models is required to produce the inverted metamorphic gradient in Ullsfjord. Both metamorphic grade and complexity of rock fabrics increase with successively higher structural levels (Figs. 8, 9) and pervasive plastic deformation is evident at only the highest structural levels. Deformation and metamorphism were concomitant and, during emplacement of the Tromsø Nappe Complex, plastic flowage was most intense at the highest structural levels where the rocks were thermally weakened. These effects lessen progressively downward. It is possible that the metamorphic gradient originally developed such that metamorphic grade decreased from west (adjacent to the structural contact with the Tromsø Nappe Complex) to east and that, during thrusting, the Balsfjord Group underwent small-scale synmetamorphic reshuffling and stacking along foliation surfaces, to produce a more vertical, compressed inverted metamorphic gradient.

The development of discrete zones of deformational fabric and corresponding metamorphic grade at different times during the emplacement of the Tromsø Nappe Complex in the study area is illustrated in Fig. 13. This model is roughly similar to that proposed by Jain & Manickavasagam (1993) for an inverted metamorphic gradient in the shear zone above the Main Central Thrust of the Himalayas. In the Himalayan model, inversion of the metamorphic isograds is accomplished through homogeneously distributed ductile shearing, which resulted in S-C composite fabrics. The inversion, however, takes place in the hanging-wall block which was brought up from depths of 25–35 km. In Ullsfjord, heat was transferred from the hanging wall Tromsø Nappe Complex, concomitant with shearing in the uppermost units of the Balsfjord Group footwall block. Deformational/metamorphic zones along the preserved shallow-dipping contact should have developed both vertically and laterally such that metamorphic grade within the Balsfjord Group increased with increasing elevation and to the west.

Summary

Structural, metamorphic and geochronological data from Ullsfjord support a model in which the main deformational event occurred during emplacement of the Tromsø Nappe Complex upon rocks of the Balsfjord Group. Fossil evidence documents that deposition and lithification of the Balsfjord units occurred during Late-Ordovician to Early-Silurian (Llandoverian) time (Bjørlykke & Olaussen 1981). Nappe emplacement and associated heat transfer resulted in prograde metamorphism of the Balsfjord Group at ca. 432 Ma, as evidenced by $^{40}Ar/^{39}Ar$ muscovite cooling ages. The fossil and metamorphic cooling ages imply that emplacement of the Tromsø Nappe Complex took place over a very short (approximately 6 MY) time span. This is consistent with data reported by Coker (1993) and Coker et al. (1995) for areas south of Ullsfjord. Deformation and metamorphism within the Lyngen Nappe Complex are interpreted to be the result of downheating from the thrust-emplaced, hot Tromsø Nappe Complex (as suggested by Krogh et al. 1990) combined with local shearing effects and small-scale reshuffling of fabrics. This resulted in the formation of the inverted metamorphic gradient within the upper units of the Balsfjord Group.

Acknowledgements. – This work was supported by the Geological Society of America (4656-91 J. Coker), Sigma Xi (99749 J.Coker), the Gulf Coast Association of Geological Societies (J. Coker), the Alabama Academy of Sciences (J. Coker), NATO (CRG.910041 to M. G. Steltenpohl), the Donors of the Petroleum Research Fund administered by the American Chemical Society (ACS-PRF 23762-GB2 M. G. Steltenpohl) and the Norwegian Marshall Foundation (M. G. Steltenpohl). We extend our thanks to Mick Kunk, US Geological Survey, Reston, VA, for arranging mass spectrometer time, Auburn University for technical support, Per Hilton and Willy Hemmingsen of Sjursnes for hospitality and logistical support and Ron Letcher at the University of Alabama at Birmingham for oversteepening himself more than once for the sake of an outcrop. We are indebted to Bruce C. Panuska, Mississippi State University, for his critical review of the initial manuscript. NGT reviewers P. G. Andreasson, S. Elvevold, and E. J. Krogh are also thanked for their very detailed reviews.

Manuscript received December 1999

References

Andresen, A. & Bergh, S. 1985: Stratigraphy and tectonometamorphic evolution of the Ordovician-Silurian Balsfjord Group, Lyngen Nappe, north Norwegian Caledonides. *In* Gee, D. G. & Sturt, B. A. (eds.): *The Caledonide Orogen – Scandinavia and Related Areas*, 579–591. Wiley and Sons, Chichester.

Andresen, A. & Steltenpohl, M. G. (eds.) 1991: A Geotraverse excursion through the Scandinavian Caledonides: Tornetrask–Ofoten–Tromsø. *Tromsø, IGCP Correlation Project 233,* 132.

Andresen, A. & Steltenpohl, M. G. 1994: Evidence for ophiolite obduction, terrane accretion and polyorogenic evolution of the north Scandinavian Caledonides. *Tectonophysics 231,* 59–70.

Andresen, A., Fareth, E., Bergh, S., Kristensen, S. E. & Krogh, E. 1985: Review of Caledonian lithotectonic units in Troms, north Norway. *In* Gee, D. G. & Sturt, B. A. (eds.): *The Caledonide Orogen – Scandinavia and Related Areas*, 569–578. Wiley and Sons, Chichester.

Barker, A. J. 1986: The geology between Salangsdalen and Gratangenfjord, Troms, Norway. *Norges geologiske undersøkelse 405,* 41–56.

Bergh, S. G. & Andresen, A. 1985: Tectonometamorphic evolution of the allochthonous rocks between Malangen and Balsfjord, Troms, north Norway. *Norges geologiske undersøkelse 401,* 1–34.

Binns, R. E. 1978: Caledonian nappe correlation and orogenic history in Scandinavia north of lat 67°N. *Bulletin of the Geological Society of America 89,* 1475–1490.

Binns, R. E. & Matthews, D. W. 1981: Stratigraphy and structure of the Ordovician-Silurian Balsfjord Supergroup, Troms, North Norway. *Norges geologiske undersøkelse 365,* 39–54.

Bjørlykke, A. & Olaussen, S. 1981: Silurian sediments, volcanics and mineral deposits in the Sagelvvatn area, Troms, north Norway. *Norges geologiske undersøkelse 365,* 1–38.

Carmichael, D. M. 1978: Metamorphic bathozones and bathograds: a measure of the depth of post-metamorphic uplift and erosion on the regional scale. *American Journal of Science 278,* 769–797.

Coker, J. 1993: Structural, petrological and geochronological studies of exotic terranes of the Troms region, Norway. Unpublished M.S. thesis, Auburn University, Ala, USA, 183 pp.

Coker, J. E., Steltenpohl, M. G., Andresen, A., Gromet, L. P. & Kunk, M. J. 1992: U-Pb and $^{40}Ar/^{39}Ar$ thermochronology and tectonic evolution of the Ofoten-Troms region, north Norwegian Caledonides. *Geological Society of America Abstracts with Programs 24,* A235–A236. Abstract.

Coker, J. E., Steltenpohl, M. G., Andresen, A. & Kunk, M. J. 1995: $^{40}Ar/^{39}Ar$ thermochronology of the Ofoten-Troms region: Implications for terrane amalgamation and extensional collapse of the north Norwegian Caledonides. *Tectonics 14,* 435–447.

Crawford, M. L., Hollister, L. S. & Woodsworth, G. J. 1987: Crustal deformation and regional metamorphism across a terrane boundary, Coast Plutonic Complex, British Columbia. *Tectonics 6,* 343–361.

Dallmeyer, R. D. 1988: Polyorogenic $^{40}Ar/^{39}Ar$ mineral age record within the Kalak Nappe Complex, northern Scandinavia. *Journal of the Geological Society of London 145,* 705–716.

Dallmeyer, R. D. & Andresen, A. 1992: Polyphase tectonothermal evolution of exotic Caledonian nappes in Troms, Norway: Evidence from $^{40}Ar/^{39}Ar$ mineral ages. *Lithos 29,* 19–42.

Deer, W. A., Howie, R. A. & Zussman, J. 1991: *An Introduction to the Rock-forming Minerals.* 528 pp. Longman Scientific and Technical, New York.

Duebendorfer, E. M. 1988: Evidence for an inverted metamorphic gradient associated with a Precambrian suture, southern Wyoming. *Journal of Metamorphic Geolology 6,* 41–63.

England, P. & Molnar, P. 1993: The interpretation of inverted metamorphic isograds using simple physical calculations. *Tectonics 12,* 145–157.

Furnes, H. & Pedersen, R. B. 1995: The Lyngen Magmatic Complex: Geology and geochemistry. *Geonytt 22,* 30.

Gee, D. G. 1975: A tectonic model for the central part of the Scandinavian Caledonides. *American Journal of Science 275A,* 468–515.

Graham, C. M. & England, P. C. 1976: Thermal regimes and regional metamorphism in the vicinity of overthrust faults: an example of shear heating and metamorphic zonation from southern California. *Earth and Planetary Science Letters 31,* 142–153.

Gustavson, M. 1966: The Caledonian mountain chain of the southern Troms and Ofoten areas, Part I: basement rocks and Caledonian metasediments. *Norges geologiske undersøkelse 239,* 162.

Himmelberg, G. R., Brew, D. A. & Ford, A. B. 1991: Development of inverted metamorphic isograds in the western metamorphic belt, Juneau, Alaska. *Journal of Metamorphic Geology 9,* 165–180.

Hodges, K. V. 1985: Tectonic stratigraphy and structural evolution of the Efjord–Sitasjaure area, northern Scandinavian Caledonides. *Norges geologiske undersøkelse 399,* 41–60.

Hoschek, G. 1969: The stability of staurolite and chloritoid and their significance in metamorphism of pelitic rocks. *Contributions to Mineralogy and Petrology 22,* 208–232.

Hubbard, M. S. 1989: Thermobarometric constraints on the thermal history of the Main Central Thrust zone and Tibetan Slab, eastern Nepal Himalaya. *Journal of Metamorphic Geology 7,* 19–30.

Hubbard, M. S. & Harrison, T. M. 1989: $^{40}Ar/^{39}Ar$ age constraints on deformation and metamorphism in the Main Central Thrust zone and Tibetan Slab, eastern Nepal Himalaya. *Tectonics 8,* 865–880.

Humphreys, R. J. 1981: The geology of northwest Ullsfjord, Troms, Norway and its regional Caledonian implications. Unpublished Ph.D. thesis, University of Wales, 342 pp.

Jain, A. K. & Manickavasagam, R. M. 1993: Inverted metamorphism in the intracontinental ductile shear zone during Himalayan collision tectonics. *Geology 21(5),* 407–414.

Krogh, E. J., Andresen, A., Bryhni, I., Broks, M. & Kristensen, S. E. 1990: Eclogites and polyphase P-T cycling in the Caledonian Uppermost Allochthon in Troms, northern Norway. *Journal of Metamorphic Geology 8,* 289–309.

Landmark, K. 1973: Beskrivelse til de geologiske kart 'Tromsö' og 'Målselv'. II. Kaledonske bergarter. *Tromsö Museums Skrifter 15,* 1–263.

Linstrøm, M. & Andresen, A. 1995: Rb-Sr dating of a syn-tectonic granite within the Lyngen Nappe Complex and its implications for late orogenic evolution of the Troms Caledonides. *Norsk Geologisk Tidsskrift 75,* 31–36.

Minsaas, O. & Sturt, B. A. 1985: The Ordovician-Silurian clastics sequence overlying the Lyngen Gabbro Complex, and its environmental significance. *In* Gee, D. G. & Sturt, B. A. (eds.): *The Caledonide Orogen – Scandinavia and Related Areas*, 379–393. Wiley and Sons, Chichester.

Munday, R. J. C. 1970: The geology of the northern part of the Lyngen peninsula, Troms, Norway. Ph.D. thesis, University of Newcastle, 216 pp.

Munday, R. J. C. 1974: The geology of the northern half of the Lyngen peninsula, Troms, Norway. *Norsk Geologisk Tidsskrift 54,* 49–62.

Padget, P. 1955: The geology of the Caledonides of the Birtavarre region, Troms, northern Norway. *Norges geologiske undersøkelse 192,* 1–107.

Peacock, S. M. 1987: Creation and preservation of Subduction-related inverted metamorphic gradients. *Journal of Geophysical Research 92,* 12673–12781.

Peacock, S. M. 1988: Inverted metamorphic gradients in the westernmost Cordillera. *In* Ernst, W. G. (ed.): *Metamorphism and Crustal Evolution of the Western United States*, 953–974. Prentice Hall, Rubey Volume VII, Englewood Cliffs.

Peacock, S. M. & Norris, P. J. 1989: Metamorphic evolution of the Central Metamorphic Belt, Klamath Province, California: an inverted metamorphic gradient beneath the Trinity peridotite. *Journal of Metamorphic Geology 7,* 191–209.

Randall, B. A. O. 1971: An outline of the geology of the Lyngen peninsula, Troms, Norway. *Norges geologiske undersøkelse 269,* 68–71.

Roberts, D. & Gee, D. G. 1985: An introduction to the structure of the Scandinavian Caledonides. *In* Gee, D. G. & Sturt, B. A. (eds.): *The Caledonide Orogen – Scandinavia and Related Areas*, 55–68. Wiley and Sons, Chichester.

Ruppel, C. & Hodges, K. V. 1994: Pressure-temperature-time paths from two-dimensional thermal models: Prograde, retrograde, and inverted metamorphism. *Tectonics 13,* 17–44.

Spear, F. S. 1993: Metamorphic phase equilibria and pressure-temperature-time paths. *Mineralogical Society of America Monograph.* 799 pp.

Steltenpohl, M. G., Andresen, A. & Tull, J. F. 1990: Lithostratigraphic correlation of the Salangen (Ofoten) and Balsfjord (Troms) Groups: evidence for the post-Finnmarkian unconformity, North Norwegian Caledonides. *Norges geologiske undersøkelse 418,* 61–77.

Streckeisen, A. 1976: To each plutonic rock its proper name. *Earth Science Reviews 12,* 1–33.

Sutter, J. F., Ratcliffe, N. M. & Mukasa, S. B. 1985: $^{40}Ar/^{39}Ar$ and K-Ar data bearing on the metamorphic and tectonic history of western New England. *Bulletin of Geological Society of America 96,* 123–136.

Tilke, P. G. 1986 *Caledonian structure, metamorphism, geochronology, and tectonics of the Sitas–Singas area, Sweden. Ph.D. dissertation, Massachusetts Institute of Technology,* 295.

Wagner, M. E. & Srogi, L. 1987: Early Paleozoic metamorphism at two crustal levels and a tectonic model for the Pennsylvania–Delaware Piedmont. *Bulletin of Geological the Society of America 99,* 113–126.

Winkler, H. G. F. 1979: *Petrogenesis of Metamorphic Rocks*. 348 pp. Springer-Verlag, New York, Heidelberg, Berlin.

Zwaan, K. B., Fareth, E. & Grogan, P. W. 1998: Geologisk kart over Norge, berggrunnskart Tromsø 1:250,000. *Norges geologiske undersøkelse.*

Appendix

$^{40}Ar/^{39}Ar$ analytical techniques

Minerals were separated by ultrasonic cleaning, heavy liquid separation, hydraulic separation and magnetic separation techniques. Optically pure separates (> 99% purity for muscovite and biotite, and no less than 99.9% purity for hornblende) were encapsulated in foil packets, together with aliquots of the monitor minerals Mmhb-1 and NJ-Biotite, and sealed under vacuum in fused silica vials. The sample vials were sealed into an aluminum irradiation can and irradiated at the US Geological Survey TRIGA reactor (Dalrymple et al. 1981) in Denver, CO. After irradiation, the samples and monitors were placed in the side-arm of a low blank double-vacuum furnace, similar to that described by Staudacher et al. (1978). After melting the tin packaging at 350°C, samples were either fused or heated incrementally to extract their argon. The gas was cleaned using SAES St707, St101, and titanium metal getters before analysis in a VG 1200b rare gas mass spectrometer for their argon isotopic composition. (Use of tradenames is for descriptive purposes only and does not imply endorsement by the US Geological Survey.) The data were reduced using the computer program ArAr* (Haugerud & Kunk 1989). Blank corrected isotopic ratios were adjusted for the effects of mass discrimination and production of interfering isotopes according to Dalrymple and others (1981). Decay constants are those recommended by Steiger & Jäger (1977). The age used for Mmhb-1 is 519.4 ± 2.5 Ma (Alexander et al. 1978; Dalrymple et al. 1981); the age used for NJ Biotite is 804.5 Ma. Plateau ages calculated by ArAr* (Haugerud & Kunk 1989) follow the definition suggested by Fleck and others (1977). The method for calculating ages and errors as well as plateau ages is discussed in Haugerud & Kunk (1989). Criteria for reliable correlation ages include a mean standard weighted deviation (MSWD) of less than 2.0, a correlation age younger than the apparent age of the saddle-minimum increment and a substantial amount of gas, evolved for the increments to which correlation is applied.

Appendix Table 1.

v 06/13/92 — 06:20:05 26 Jan 1993

s-184 Hornblende #3RD65

J = 0.009050 = 0.50% — Sample wt. = 0.1015 g

TEMP °C	Initial & radiogenic ^{40}Ar	Potassium-derived ^{39}Ar	Chlorine-derived ^{38}Ar	Calcium-derived ^{37}Ar	Initial ^{36}Ar	Age* in Ma	**
1050	1.857E-11	5.649E-13	7.494E-14	5.737E-12	1.201E-15	461.82*	1.15
1075	5.190E-12	1.647E-13	2.053E-14	1.652E-12	***	449.57*	0.92
TOTAL GAS	2.376E-11	7.296E-13	9.547E-14	7.389E-12	1.334E-15	459.07	

Appendix Table 2.

v 06/13/92 — 05:12:38 26 Jan 1993

s-184 Muscovite #61RD85

J = 0.009319 = 0.50% — Sample wt = 0.1018 g

TEMP °C	Initial & radiogenic ^{40}Ar	Potassium derived ^{39}Ar	Chlorine derived ^{38}Ar	Calcium derived ^{37}Ar	Initial ^{36}Ar	AGE* in Ma	**
850	2.754E-11	9.057E-13	2.263E-15	***	1.874E-15	442.06*	0.96
900	1.073E-10	3.563E-12	***	***	3.994E-15	441.78*	0.32
950	8.935E-11	2.992E-12	***	***	1.434E-15	441.02*	0.36
1000	4.018E-11	1.349E-12	***	***	***	438.99*	0.74
1050	2.417E-11	8.058E-13	***	***	***	441.72*	2.27
1100	3.479E-11	1.168E-12	***	***	***	439.38*	1.10
1150	7.537E-11	2.523E-12	***	***	1.647E-15	440.53*	0.25
1200	3.829E-11	1.279E-12	***	***	***	442.41*	0.64
1250	9.852E-12	3.267E-13	***	***	***	444.79*	1.88
TOTAL GAS	4.468E-10	1.491E-11	3.846E-15	1.855E-15	1.185E-14	441.11	

50.0% of gas on plateau, steps 850 through 950 PLATEAU AGE = 441.48 + 2.19
59.3% of gas on plateau, steps 950 through 1150 PLATEAU AGE = 440.52 + 2.18

Appendix Table 3.

v 06/13/92 — 04:33:07 26 Jan 1993

M-9 Muscovite #55RD85

J = 0.009319 = 0.50% — Sample wt = 0.1025 g

TEMP °C	Initial & radiogenic ^{40}Ar	Potassium-derived ^{39}Ar	Chlorine-derived ^{38}Ar	Calcium-derived ^{37}Ar	Initial ^{36}Ar	AGE* in Ma	**
900	2.034E-11	6.911E-13	***	4.793E-15	***	433.17*	1.20
950	4.955E-11	1.675E-12	2.842E-15	5.844E-15	2.948E-15	432.33*	0.56
1050	1.018E-10	3.471E-12	***	5.902E-14	3.552E-15	432.01*	0.45
1100	5.175E-11	1.763E-12	***	2.402E-14	2.133E-15	431.54*	0.94
1150	6.726E-11	2.349E-12	***	2.494E-14	1.986E-15	423.29*	10.51
1200	2.961E-11	1.005E-12	***	1.973E-14	***	435.14*	1.30
TOTAL GAS	3.203E-10	1.095E-11	3.695E-15	1.384E-13	1.195E-14	430.48	

90.8% of gas on plateau, steps 900 through 1150 PLATEAU AGE = 432.14 + 1.93

All gas quantities are in moles. No blank correction.
* Ages calculated assuming initial $^{40}Ar/^{36}Ar$ = 295.5 = 0
** 1-sigma precision estimates are for intra-sample reproducibility.
** 1-sigma precision estimates for plateaux are for intra-irradiation package reproducibility.
*** Below detection limit.

References

Alexander Jr., E. C., Mickelsom, G. M. & Lamphyre, M. A. 1978: Mmhb-1: A new $^{40}Ar/^{39}Ar$ dating standard. *Journal of Geophysical Research 94,* 17917–17935.

Dalrymple, G. B., Alexander, E. C., Lanphere, M. A. & Kraker, G. P. 1981: Irradiation of samples for $^{40}Ar/^{39}Ar$ dating using the Geological Survey TRIGA Reactor. *U.S. Geological Survey Professional Paper 1176,* 55 pp.

Fleck, R. J., Sutter, J. F. & Elliot, D. H. 1977: Interpretation of discordant $^{40}Ar/^{39}Ar$ age spectra of Mesozoic tholeiites from Antarctica. *Geochimica et Cosmochimica Acta 41,* 15–32.

Haugerud, R. A. & Kunk, M. J. 1989: ArAr* A computer program forreduction of $^{40}Ar/^{39}Ar$ data. *U.S. Geological Survey Open File Report 99–261,* 68 pp.

Staudacher, T. H., Jessberger, E. K., Dorflinger, D. & Kiko, J. 1978: A refined ultra-high-vacuum furnace for rare gas analysis. *Journal of Physical Earth Science Instruments 11,* 781–784.

Steiger, R. H. & Jäger, E. 1977: Subcommission on geochronology: Convention on the use of decay constants in geo- and cosmochronology. *Earth and Planetary Science Letters 36,* 359–362.